1996A&A...308..643D

Astron. Astrophys. 308, 643–655 (1996)

ASTRONOMY AND ASTROPHYSICS

Quasi-Separatrix layers in solar flares

I. Method

P. Démoulin[1], J.C. Hénoux[1], E.R. Priest[2] and C.H. Mandrini[3]

[1] Observatoire de Paris, DASOP, URA326 (CNRS), F-92195 Meudon Cédex, France
[2] Mathematical and Computational Sciences Dept, The University, St Andrews, KY16 9SS, Scotland, UK
[3] Instituto de Astronomía y Física del Espacio, IAFE-CONICET, CC.67, Suc.28, 1428 Buenos Aires, Argentina*

Received 10 May 1995 / Accepted 31 August 1995

Abstract. Magnetic reconnection is usually thought to be linked to the presence of magnetic null points and to be accompanied by the transport of magnetic field lines across separatrices, the set of field lines where the mapping of field lines is discontinuous. In view of the variety of observed flaring configurations, we show that this view is too restrictive. Instead, Priest and Demoulin (1995) have explored a way of generalising the concept of separatrices to magnetic configurations without field-line linkage discontinuities. They propose that magnetic reconnection may also occur in 3D in the absence of null points at "quasi-separatrix layers" (QSLs), which are regions where there is drastic change in field-line linkage. In previous studies we have shown that solar flare kernels are linked to the topology of the active-region magnetic field. The observed photospheric field was extrapolated to the corona using subphotospheric magnetic sources and the topology was defined by the magnetic linkage between these sources, the method being called SM (for Source Method). In this paper we define a new method, called QSLM (for Quasi-Separatrix Layers Method), which finds the location of QSLs above the photosphere. It is designed to be applied to any kind of magnetic field representation, while, in the present paper, we apply it only to simple theoretical magnetic configurations in order to compare it with the SM. It generalises the concept of separatrices to magnetic configurations without field-line linkage discontinuities. The QSLM determines elongated regions that are in general located along small portions of the separatrices defined by the SM, and in the limit of very concentrated photospheric fields both methods give the same result. In bipolar magnetic configurations two QSLs are found at both sides of the inversion line, while in quadrupolar configurations four appear. We find that there is a wide range for the thickness of the QSLs, which is determined by the character (bipolar or quadrupolar) of the magnetic region and by the sizes of the photospheric field concentrations. We then show that smooth photospheric motions induce concentrated currents at the locations defined by the QSLM. We prove this only for initially potential configurations but, due to the form of the equations, we conjecture that it is also valid for any kind of initial magnetic equilibrium. We conclude that, even in bipolar configurations, there are localized places where current build-up can be induced by photospheric motions, leading to ideal MHD breakdown with strong flows and magnetic energy release.

Key words: magnetic fields – Magnetohydrodynamics (MHD) – Sun: flares – Sun: magnetic fields

1. Introduction

The energy needed to heat the solar corona and to power flares is thought to come from the coronal magnetic field, since its free energy dominates all other forms of stored energy. However, because the medium is a plasma with a high magnetic Reynolds number, the magnetic energy cannot be released fast enough (by more than 10 orders of magnitude for a typical coronal scale-length of 10-100 Mm). In this context the magnetic configurations where a smooth evolution at the boundaries leads to the formation of current sheets play a key role. Because small scale lengths are created, the resistive term in the induction equation becomes important and magnetic energy can be released fast enough. In ideal MHD, the formation of current sheets in 2D potential magnetic configurations with an X-point has been known for a long time (see the reviews of Amari 1991 and Van den Oord 1993). It has been argued that a current sheet can store enough magnetic energy to power a flare (Somov 1986, 1992 and references therein). At some point in the evolution, this current sheet becomes unstable and turbulence develops increasing the plasma resistivity. Then the stored energy is rapidly released giving a flare (e.g. Heyvaerts et al, 1977). It has instead been argued that reconnection tends to occur at a rate imposed by the magnetic field evolution (Priest & Forbes 1992b). In this

Send offprint requests to: P. Démoulin
* Member of the Carrera del Investigador Científico, CONICET

© European Southern Observatory • Provided by the NASA Astrophysics Data System

1996A&A...308..643D

other case the current in the sheet is always small and magnetic energy is instead stored in smooth field-aligned currents, such as a twisted flux tube, at a spatial scale length (typically 1-10 Mm) that gives a negligible role to the resistive term. In this evolution an ideal instability or nonequilibrium occurs forcing reconnection to take place at the separator (Priest and Forbes, 1990). Another possibility is that the field-aligned currents are formed by photospheric or convective motions and then carried towards the locations of current sheets where the stored energy can be rapidly released. Present observations are not able to discriminate between these three kinds of evolution, but they do show the importance of the magnetic topology (Démoulin 1994).

The 3D characteristics of magnetic reconnection are highly complex and are only just beginning to be understood (Schindler et al, 1988; Priest and Forbes, 1989, 1992a; Lau and Finn, 1990; Priest and Titov, 1995). When the magnetic configuration is described by a series of sources it is possible to generalise the 2D picture in a straightforward way. The separatrix surfaces divide up the volume into topologically distinct regions in the sense that a particular region contains only field lines that start at a particular source and end up at another particular source; when reconnection occurs, magnetic flux is transferred across the separatrices from one region to another. Following this line, several studies (Gorbachev & Somov, 1988, 1989; Mandrini et al. 1991, 1993, 1995; Démoulin et al. 1993, 1994b; Van Driel-Gesztelyi et al. 1994) have related the flare ribbons to the magnetic topology deduced from the observed photospheric field by using subphotospheric magnetic sources. The topology has been defined by the magnetic link between these sources, using a method called SM (for Source Method). Hα flare brightenings and current concentrations have been found on the intersection of the separatrices with the chromosphere and being magnetically connected by field lines passing close to the separator. This happens for a variety of observed magnetic configurations, from quadrupolar regions to bipolar ones with an "S" shaped inversion line and even to bipolar regions with a nearly potential field and an almost straight inversion line. The first case is a direct extension to 3D of a 2D magnetic configuration with an X-point (as used in 2D reconnection), while the second and third seem at first closer to a simple arcade model ! Some flaring active regions contain null points above the photosphere, especially when a new, almost oppositely directed, bipolar region emerges between the two main polarities of a sunspot group. However, other active regions contain no such null points (Démoulin et al. 1994a). Therefore, it seems that the way in which the separatrices of active regions are defined needs to be changed to take into account what is common to all observed flaring configurations.

Separatrices are surfaces where the mapping is discontinuous. On the other hand, we have shown in a recent paper (Priest and Démoulin, 1995; hereafter Paper I) that magnetic reconnection may occur in 3D at so-called "quasi-separatrix layers" (QSLs) for a larger ensemble of magnetic configurations than that when null points or field lines tangent to the boundary are present. This concept refers to surfaces where there is a steep gradient or a drastic change in the mapping of field lines from one boundary to another of a given magnetic configuration. We have suggested that magnetic reconnection occurs when there is a breakdown of ideal MHD and a change of the connectivity of plasma elements, where the field-line velocity becomes much larger than the plasma velocity so that the field lines slip through the plasma, and we have shown that this breakdown can occur in 3D in the QSLs with an electric field component parallel to the magnetic field. In this paper we present a new method, called QSLM (for Quasi-Separatrix Layers Method), for computing the connectivity of flaring configurations.

The Quasi-Separatrix Layers Method is based on finding regions where drastic changes in field-line linkage occur above the photosphere and it is presented in Sect. 2. In Sect. 3 we apply both methods to the simple potential magnetic configurations given by four magnetic sources, which represent the typical structure of observed flaring regions. We compare the QSLM to the SM previously used, showing that the new method constrains even more the probable location of energy release. Then we justify the selected method compared to other possibilities and we investigate the shape and thickness of the QSLs in both quadrupolar and bipolar regions, showing in particular that they have different observed signatures for the ribbon locations. Next, we investigate, in Sect. 4, the storage of magnetic energy, showing that field-aligned concentrated currents are generally formed by smooth photospheric motions at the locations of the QSLs. Conclusions on flare mechanisms are then given in Sect. 5.

2. Numerical methods to determine the magnetic field connectivity

2.1. Source method

The topology of a magnetic configuration is a global property and its determination requires the computation and analysis of a large number of field lines (see the discussion in the Appendix). Baum and Bratenahl (1980) and Gorbachev & Somov (1988, 1989) calculated numerically the topology of the potential field created by four magnetic poles. The next step, to represent in a better way the observed magnetic field, was to introduce many sources (Mandrini et al. 1991, 1993) and to determine their positions and intensities fitted by least squares to the observed magnetic data (Démoulin et al. 1994b). In these cases many separatrices can be present and the sources should be gathered in groups (for example, all sources used to describe the observed complex shape of a magnetic field concentration belong to the same group). The connectivity of a field line is defined by the groups to which the sources, found at both of its ends, belong. On these complex configurations a trial and error method, based in field-line drawing, is not suitable to find the location of separatrices and so an automatic algorithm called SM (Démoulin et al. 1992) was developed. This method seems at first sight to depend strongly on the type of sources (poles or dipoles) used. In fact even for complex regions a pole or a dipole representation gives the same topology when the number of sources is great enough. In practice a number of sources $\leq$ 20 is suffi-

© European Southern Observatory • Provided by the NASA Astrophysics Data System

1996A&A...308..643D

cient for all the regions studied, considering the precision of the observations and the limitations of the photospheric field extrapolation (Démoulin et al. 1994b). We have also shown that magnetic poles are a good approximation to the field created by subphotospheric elongated flux tubes, which are likely to be present in the convective zone.

When computing the field-line connectivity with the SM, one needs to integrate below the photosphere where a magnetic field model is not available. Therefore, the pole or dipole representations consider the concentration of the field at subphotospheric layers in a crude way. However, the field-line path below the photosphere has a negligible length because the observed photospheric field concentrations have smaller sizes than the typical distance between them. This is probably the reason why the SM succeeded in locating flare brightenings on the separatrices. However, the SM cannot be used with other magnetic-field extrapolation techniques such as Fourier transform, relaxation or MHD codes because it intrinsically needs sources to define the magnetic connectivity. Then, it is worth developing a method that takes into account the field-line linkage above the photosphere only.

2.2. *How can we define the connectivity for a 3D magnetic field ?*

In 2D configurations the magnetic topology is defined by the presence of discontinuities in field-line linkage. The complexity of the mapping of field lines is reduced to the properties of one function, the flux function. A constant value of the flux function defines the limit between different connectivity volumes or cells; this constant is the value of the flux function at null points or at field lines tangent to the boundary. In 3D the magnetic topology has been traditionally defined in terms of the presence of null points in the field or of field lines tangent to the boundary (the photosphere in our case). The field line connecting two nulls, called the separator, is the generalisation to 3D of a 2D X-point. Field lines in its vicinity connect to four distinct regions. The field-line linkage is discontinuous across two surfaces, called separatrices, which intersect at the separator.

In 2D and $2\frac{1}{2}$D magnetic reconnection takes place at null points with flux transfer across the separatrices. However, in 3D a debate exists on how to define magnetic reconnection and, in particular, under which circumstances it occurs (see Hesse & Schindler 1988, Lau & Finn 1990, Priest & Forbes 1992a, Priest and Titov, 1995). As a first approach, it seems natural to extend the 2D models to 3D and therefore to look for discontinuities in field-line linkage (see Bungey et al. 1995 for example). We will show in Sect. 3 that a discontinuity in field-line linkage is present only when the photospheric field of a region with four sources is quadrupolar ($-+-+$). Some flaring regions have this property and some do not (Démoulin et al. 1994a). In fact a direct generalization of the definition of topology from 2D to 3D would exclude many magnetic configurations that are seen to flare !

In previous studies we have shown that the observed flare brightenings are located on the separatrices computed with the SM. Does this mean that the path of field lines (and so the presence of nulls) below the photosphere is important for the flaring process ? We have argued, based on the high inertia of the photosphere, that this should not be the case: flares are coronal events with negligible effects on subphotospheric layers. At this point we feel that the magnetic topology is important in flares; but we need to characterise the connectivity of the coronal field, in a general way, without any reference to null points or field lines tangent to the photosphere; however, this definition should include these as particular cases.

2.3. *Quasi-Separatix layers method*

In $2\frac{1}{2}$D models (Low 1987, 1992, Low & Wolfson 1988, Wolfson 1989, Vekstein et al. 1991, Vekstein & Priest 1992, Billinghurst et al. 1993) discontinuities in field-line linkage at the boundary are the origin of the formation of current sheets. In our topological studies of flaring regions (see references in the Introduction) we have found that observed flare brightenings are located where the field-line linkage looks "discontinuous" above the photosphere. However, as discussed in Sect. 2.2 and as will be shown in Sect. 3, to develop a method to find regions with only this characteristic is too restrictive. We will rather develop a general method to look for regions where there is a drastic change in field-line linkage above the photosphere, a discontinuous change being a particular case. These regions have been called QSLs in Paper I and, as shown there, are the places where 3D magnetic reconnection may occur in the absence of null points.

We are interested in locating the region where a drastic change in field-line linkage occurs, i.e. where field lines initially close to one another separate widely over a short distance. Let us integrate the field line passing at through point P(x, y, z) of the corona in both directions over a distance s along the field line. The points (x', y', z') and (x'', y'', z''), which are the coordinates of the two end points, define a vector $\boldsymbol{D}(x, y, z) = \{X_1, X_2, X_3\} = \{x'' - x', y'' - y', z'' - z'\}$. A drastic change in field-line linkage means that for a slight shift of point P(x, y, z), $\boldsymbol{D}(x, y, z)$ varies greatly. The norm $\tilde{N}$, defined by

$$\tilde{N}(x, y, z, s) = \sqrt{\sum_{i=1,3} \left[\left(\frac{\partial X_i}{\partial x} \right)^2 + \left(\frac{\partial X_i}{\partial y} \right)^2 + \left(\frac{\partial X_i}{\partial z} \right)^2 \right]}, \quad (1)$$

allows us to locate the region of drastic change in connectivity for a given value of s. Physically s can be limited either by a boundary or by the distance reached by waves during the reconnection process, say s_w. This definition looks well suited for magnetic regions where field lines do not reach a boundary (as in tokamaks) or when the reconnection process takes place in a time shorter than the time needed for the information at the boundary to reach the reconnecting region (as in the Earth's magneto-tail or in impulsive flares with fine temporal-structures). In cases of line-tying to boundary, the relevant s should be the mimimum of s_w and the distance to the boundary.

© European Southern Observatory • Provided by the NASA Astrophysics Data System

1996A&A...308..643D

In many solar flares, the whole process takes place in the fraction of an hour or in several hours, which is much longer than the Alfven crossing time for the whole structure, so the distance to the photosphere is the appropriate one, so $z' = z'' = 0$, say, and Eq. (1) simplifies to:

$$\tilde{N}(x,y,z) = \sqrt{\sum_{i=1,2}\left[\left(\frac{\partial X_i}{\partial x}\right)^2 + \left(\frac{\partial X_i}{\partial y}\right)^2 + \left(\frac{\partial X_i}{\partial z}\right)^2\right]}. \quad (2)$$

However, due to the presence of the partial derivative with respect to z this norm is singular on the inversion line of the normal field component (B_z) when the initial point (x, y, z) belongs to the photosphere. Since field lines are tangent to the boundary there, it gives very high values in the vicinity of the inversion line (infinite on the inversion line itself). This occurs not only for field lines bent up (which are called bald patches (Bungey et al. 1995) and known to define separatrices) but also for field lines bent down !

In the working approximation of an abrupt transition from a low- to a high-β plasma line-tying is imposed at the photospheric level ($z = 0$): the location in the photospheric plane of the magnetic field-line footpoints is imposed as a function of x and y (and not z). We show in Sect. 4 that the smooth evolution of these footpoints leads to the formation of localized currents at the places of drastic change in field-line linkage. These are also the probable locations of magnetic reconnection (for example, if it is induced by a current-driven instability). We then keep to the definition used in Paper I for the norm as:

$$N(x,y) = \sqrt{\sum_{i=1,2}\left[\left(\frac{\partial X_i}{\partial x}\right)^2 + \left(\frac{\partial X_i}{\partial y}\right)^2\right]}. \quad (3)$$

$N(x, y)$ is evaluated only on the boundary, reinforcing the particular role of line-tying. $N(x, y)$ is the norm of the displacement gradient tensor, defined when mapping the field lines to the boundary. The choice of this particular function, which enables us to locate the strong flows induced by small and smooth photospheric motions, is justified in Paper I and further in Sect. 3.3. The locations of high values of $N(x, y)$ define the field lines involved in the QSLs; following these field lines allows to locate the coronal part of the QSLs. We believe that $N(x, y)$ is the most appropriate function to use in magnetic configurations where line-tying to a boundary is important, while Eq. (1) is suitable for magnetic reconnection problems not involving line-tying.

$N(x, y)$ has the following properties:
- it is non-dimensional,
- it is independent of the system of coordinates,
- it adds up the variation in field-line linkage in the x- and y-directions and the locations where N is unusually large, in a sense that will be made precise in Sect. 3, corresponds to the regions called QSLs;
- it can be applied to any kind of magnetic field following a quasi-static evolution, the field no longer needs to be represented by a series of sources (as with the SM). The QSLM requires us only to know the field at all points of the studied volume.
- when the maximum value of N is not too large (so that resistive effects are negligible), we show in Sect. 4 that concentrated currents are formed at the locations of high values of N; while when N is too large, a breakdown of ideal MHD must occur.

The numerical computation of the function N requires integrating a huge number of field lines, which is computer time consuming. Therefore, as in the SM, we start with a coarse rectangular numerical grid, which allows us to have a first estimate of N at every point of the grid using centred finite differences. The n locations where N has the largest values are retained and the computation is repeated on a grid twice as fine, only at points located in the neighbourhood of the n retained points. The process is repeated until enough spatial accuracy is obtained. This results in an automatic method that computes field lines mainly where the field-line linkage changes drastically. The value of n is imposed at each iteration to have fast or precise results. We call this method QSLM.

3. Field-line linkage in typical flaring magnetic configurations

In this section we apply the two methods (SM and QSLM) to magnetic field configurations that are simple, but still representative of observed flaring regions. As was previously shown, the basic topological features are present in a model with four sub-photospheric poles. We will use the same representation as in Démoulin et al. (1994a) and will refer to Fig. 1 of that paper for the geometry of the configurations. One magnetic bipole, called the main one, is formed by two poles (1,2) and is parallel to the x-axis. It is at a depth $Z_M = -0.1$ below the photosphere and the distance between poles is normalised to unity. The other bipole, called the parasitic one, is formed by two other poles (3,4). It is characterised by the coordinates of its centre ($X_P = 0$, $Y_P = 0$, Z_P), the half-distance between poles ($R_P = 0.1$) and its orientation (polar angle $\theta_P = 90^0$ and azimuthal angle φ_P). The intensities of the poles are $e_1 = -e_2 = 1$ and $e_3 = -e_4 = e$. In Démoulin et al. (1994a), we have shown that the main parameter affecting the topology is φ_P. It is also the parameter for which we have not found a typical value in flaring regions and the one that mainly describes the path of the photospheric inversion line; that is to say, the character bipolar/quadrupolar of the regions. The other parameters are taken close to the average observed values defining a standard configuration.

3.1. *Comparison of the source method with the Quasi-Separatrix Layers Method*

In a bipolar configuration, with main and parasitic bipoles nearly aligned (say $\varphi_P = 30^0$), the gradient in field-line linkage above the photosphere is not steep because field lines have shapes similar to those in an arcade. We choose such a configuration to show: first, that the QSLM defines in fact regions where the field-line linkage changes more drastically than everywhere else; secondly, that the amplitude of the change depends strongly on the photospheric field concentration; and, finally, that the QSLM

© European Southern Observatory • Provided by the NASA Astrophysics Data System

1996A&A...308..643D

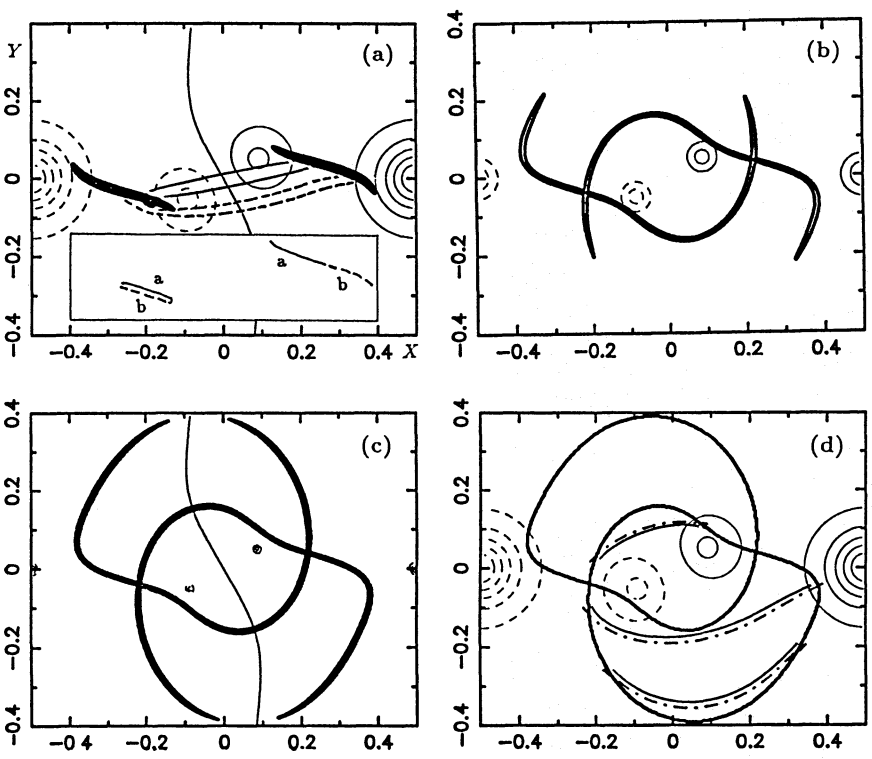


Fig. 1a–d. Comparison of the Quasi-Separatrix Layers Method (**a-c**) and Source Method (**d**) for a bipolar configuration and various photospheric field concentrations. The magnetic sources are located in a horizontal plane located at depth Z_C below the photosphere ($Z_M = Z_P = Z_C$, $\theta_P = 90^0$). The parameters of the configuration (as defined in Sect. 3) are: $X_P = Y_P = 0$, $R_P = 0.1$, $\varphi_P = 30^0$ and $e = 0.4$. The vertical photospheric magnetic field B_z is shown by equispaced isocontours (between minimum and maximum values) with thin continuous (positive), dashed (negative) and thick continuous lines (inversion line of B_z). **a-c** show an isocontour of the function N (= 5,10,10, respectively) in the plane $Z = Z_C + 0.1$ with sources at depths $Z_C = -0.1$, $Z_C = -0.05$ and $Z_C = -0.02$, respectively. The intersection of the separatrices (computed with the SM) with the plane $Z = 0$. is given by the thick continuous lines in **d**. Some field lines linking the regions of rapid change are shown in **a** as explained in the text; a sketch of the connectivity is shown in a separate box. Some other field lines are added in **d** to highlight that there is no rapid change of photospheric connectivity in the parts of the separatrices not associated with quasi-separatrix layers.

gives the same results as the SM in the limit of infinitely concentrated photospheric fields. To study the case of highly concentrated fields, all the sources have been located in the same horizontal plane, $Z = Z_C$ (so $Z_P = Z_M = Z_C$), with Z_C varying from -0.1 to -0.02. The photospheric level is at $Z = 0$. Therefore, in the limit $Z_C = 0$ the photospheric sources are infinitely concentrated. As mentioned previously the field-line integration, required to compute the function $N(x, y, z)$ in the QSLM, starts and ends at photospheric level where this function is computed for every field line. In order to facilitate a comparison between the two methods the cut shown in Figs. 1a to 1c is made at the same distance ($Z = Z_C + 0.1$) above the plane of the magnetic sources. Moreover, in order to have the same field strength in that plane as in the standard configuration, $e = 0.4$ was used.

When the photospheric field concentrations are moderate - with the sources at a depth -0.1 below the photosphere in Fig. 1a - a grid of 300 by 300 points allows a resolution of the variations in field-line linkage. The QSLM defines two elongated regions located on both sides of the inversion line. These regions have the typical shape of observed H_α ribbons in such bipolar magnetic configurations: they are hardly detectable by drawing a large number of field lines with random starting points, so a special algorithm is needed to detect them. Some selected field lines are drawn in Fig. 1a in continuous (dashed) lines to show the particular link existing between the two regions: they start from the upper (lower) border of the left region and reach the lower-left (lower-right) border of the right region. A sketch of the connectivity is shown by underlining the location of the footpoints of the field lines in a separate box in Fig. 1a (using the same drawing convention as for field lines). Parts called a (resp. b) are linked together. This fold is typical of QSLs.

Let us now analyse quantitatively the displacement of a photospheric footpoint of a field line when the position of its other footpoint is slightly changed in the photosphere. The displacement of the two footpoints is in general of the same order of magnitude ($N \approx 1$) except in localised regions where N takes high values. As shown in Fig. 1a, for a moderate concentration of the photospheric field the maximum of the function N is also moderate with $N_{max} \approx 6.2$. It becomes much more important as the concentration of the photospheric field increases and reaches $N_{max} \approx 110$ in Fig. 1b and $N_{max} \approx 440$ in Fig. 1c. For these cases it is numerically too expensive to resolve the variations of N on a 2D grid; a cut with a segment across the region of drastic change is instead used to determine its transverse size and N_{max} (cf. Sect. 3.4).

Fig. 1d shows the intersection of the separatrices computed using the SM with the plane $Z = 0$. These separatrices are recovered by the QSLM in the limit of infinitely concentrated photospheric fields ($Z_C = 0$). In this limit the field lines can end up only at isolated photospheric points and the linkage is discontinuous; this is associated with the presence of null points at photospheric level. In configurations with finite field concentrations the field-line linkage is usually continuous and there is only one connectivity cell ! However, the QSLM defines regions which are located close to portions of the separatrices computed

© European Southern Observatory • Provided by the NASA Astrophysics Data System

1996A&A...308..643D

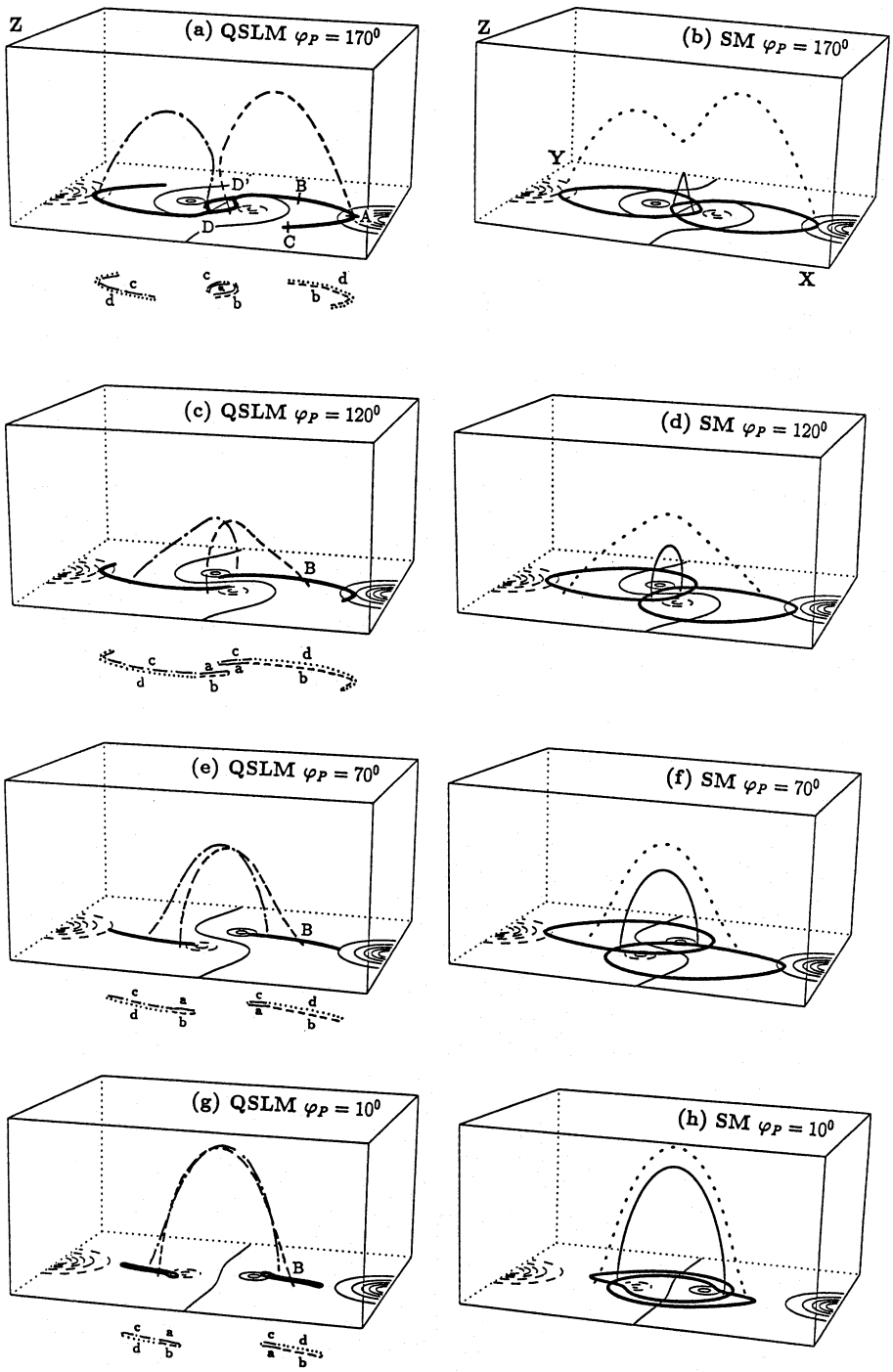


Fig. 2a–h. Results obtained with the QSLM and the SM at the photosphere for bipolar and quadrupolar regions: **a,b** $\varphi_P = 170^0$, **c,d** $\varphi_P = 120^0$, **e,f** $\varphi_P = 70^0$, **g,h** $\varphi_P = 10^0$. The drawing convention is the same as in Fig. 1. The parameters are: $Z_M = -0.1$, $X_P = Y_P = 0$, $Z_P = -0.05$, $R_P = 0.1$, $\theta_P = 90^0$, $e = 0.1$. Two pairs of field lines show the field-line linkage before and after reconnection. A sketch of the connectivity has been added with the same convention for line drawing and for field lines; parts linked together have the same lettering. Capital letters refer to particular locations of the quasi-separatrix layers (see text and following figures).

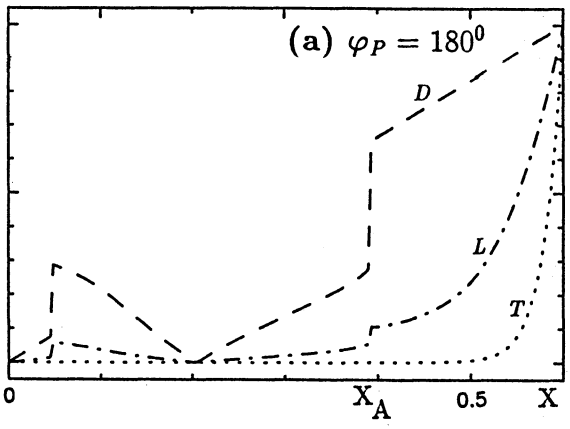
with the SM, compare Fig. 1a to Fig. 1d. The correspondence between the results of the QSLM and the SM justifies a posteriori the previous works on the topology of flaring active-regions, where integration of field lines was performed until reaching a subphotospheric source. The portions of the separatrices not found with the QSLM are regions where the field-line linkage changes slowly above the photosphere; they have no more meaning for the corona than any other locations where separatrices are not present (Fig. 1d).

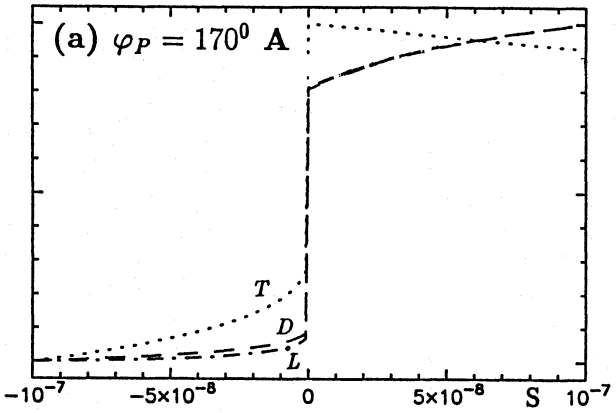
3.2. Evolution of the connectivity from quadrupolar to bipolar regions

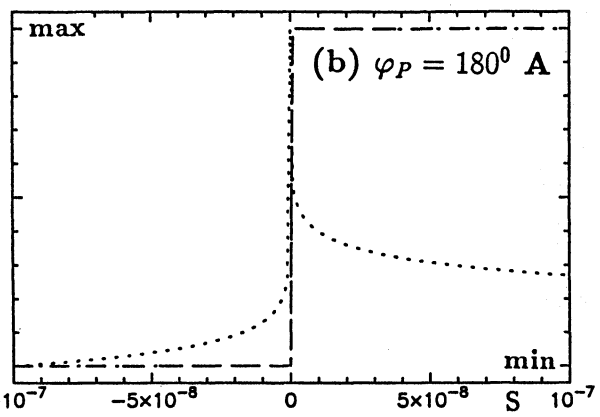
For a symmetric quadrupolar configuration with aligned sources the QSLM defines closed surfaces, just as the SM. When the alignment (or the symmetry) is slightly broken, the QSLM gives only part of the separatrices computed with the SM (Figs. 2a,b). Moreover, the QSLM detects field lines tangent to the boundary, which results in a slightly different spatial location of the computed QSLs from that of the SM separatrices (regions around

© European Southern Observatory • Provided by the NASA Astrophysics Data System

1996A&A...308..643D







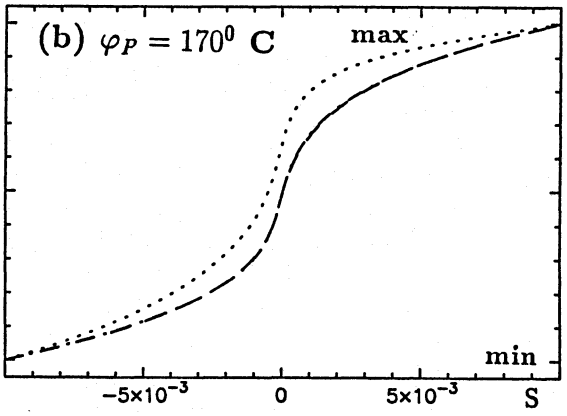


Fig. 3a and b. Evolution of the distance D between the field line foot-points (dashed curve), the field line length L (dashed dotted curve) and the delay function $T = \int ds/B$ (dotted curve) as functions of the abscissa of the initial foot-point for $\varphi_P = 180^0$ (the other parameters have their standard values, see Fig. 2). The curves have been normalized to their minimum and maximum values in the range of x values considered. The plots are performed along a segment parallel to the x-axis. **b** is a local zoom of **a** at location A (see Fig. 2a); it uses the abscissa S centred on the discontinuity location. In this quadrupolar configuration a logarithmic singularity is present in the delay function and a step one in the D and L functions (they are overlaid in this figure).

Fig. 4a and b. Plot along segments centred at points A and C (see Fig. 2a) and perpendicular to the quasi-separatrix layer. The drawing convention is the same as in Fig. 3. In this slightly asymmetric quadrupolar configuration ($\varphi_P = 170^0$) all the three functions have only jump discontinuities (e.g. point A) or are continous (e.g. point C). Functions D and L partly overlay.

points D, D' in Fig. 2a and regions connected by field lines to these points). In all the flares that we have studied so far, we have never found the flare kernels related to these tangential field lines, so the relevant regions for flaring are rather the ones shown in the sketch of Fig. 2a . It predicts in quadrupolar regions four ribbons in accordance with observations. These regions are linked two by two, as in 2D quadrupolar models. When reconnection occurs, the field lines of Fig. 2a connecting footpoints identified by letters b and c are transformed to those of Fig. 2b connecting footpoints a and d (or the reverse depending on the way reconnection is induced, by for example global instability or flux emergence).

As φ_P decreases below $\approx 170^0$ field lines tangent to the boundary disappear, as do null points above the photosphere, so the field-line linkage is no longer discontinuous but it changes drastically in a short scale length (see Sect. 3.3 below). The previous four regions of drastic change are progressively transformed, by grouping, into two elongated and folded strips (Fig. 2c,e,g). The field-line linkage is still typical of a 2D quadrupolar configuration while the photospheric field is bipolar. Reconnection transforms field lines in a similar way to quadrupolar regions (compare field lines drawn in all Figs. 2). As the parasitic bipole becomes less antiparallel to the main one, a smaller portion of the separatrices computed with the SM is found with the QSLM. But even in the near-parallel configuration ($\varphi_P \approx 10^0$), where the photospheric inversion line is almost straight and the field is potential, two elongated strips are found. Kernels with a small extension are predicted in this case.

3.3. How can we locate Quasi-Separatrix layers ?

So far we have used the function N (Eq. (3)) but other possibilities have been suggested to locate separatrices. Can we use them also to locate QSLs ? When the bipoles are nearly antiparallel ($\varphi_P \approx 180^0$) the magnetic field topology is similar to that of a $2\frac{1}{2}$D quadrupolar configuration: there are four different kinds of linkage between four distinct photospheric magnetic regions,

© European Southern Observatory • Provided by the NASA Astrophysics Data System

1996A&A...308..643D

provided that the parasitic bipole is intense enough. The location of these four regions can be determined by studying the discontinuity of three functions: the distance (D) between the photospheric footpoints of field lines, the field-line length (L) and the delay function ($T = \int ds/B$, where the integration is performed along a magnetic field line). The first two functions have a jump discontinuity and the third a logarithmic one (Fig. 3), as was shown by Lau (1993). The existence of these discontinuities is related to the presence of a magnetic null point in the corona that defines a quasi-null line, the magnetic field line connecting the null to the photosphere. This quasi-null line has properties similar to those of a separator.

However, the logarithmic discontinuity of the delay function is not a general property of flaring configurations: it disappears if the parasitic bipole is not closely antiparallel to the main one to give a jump discontinuity. On a large spatial scale the delay function has nearly the same behaviour for $\varphi_P = 170^0$ as it has for $\varphi_P = 180^0$ (Fig. 3a), but at lower scales the two are quantitatively different: compare Fig. 3b and Fig. 4a. This is natural because the logarithmic discontinuity, as mentioned previously, is linked to the presence of a null point above the photosphere, which occurs only for nearly antiparallel bipoles (Démoulin et al. 1994a). So, in general, it is not useful to look for a logarithmic discontinuity of the delay function. The jump discontinuity of the three functions (D, L, T) is also not a general property of flaring configurations: it disappears if the parasitic bipole is not nearly antiparallel to the main one (Fig. 5). However, a drastic change of the functions is still present at some locations in the configuration even in bipolar cases (like in Figs. 1, 2).

Which function should we choose to find and measure the thickness of regions where there is a steep gradient in field-line linkage ? Even for antiparallel configurations ($\varphi_P = 180^0$), the logarithmic discontinuity of the delay function can be missed easily if it is computed on a coarse grid through the whole magnetic region, as shown in Fig. 3a (but in general we do need to start by looking in the whole region). It is only when a series of field lines is computed very close to a separatrix that the logarithmic discontinuity appears (Fig. 3b). Moreover, the delay function increases abruptly when the field lines move away from the photospheric field concentrations because the field is low there (Fig. 3a). This is not related to the presence of separatrices and can be falsely interpreted as a drastic change by a numerical algorithm. For these reasons, we consider that the delay function is not adequate. A similar but less important problem appears with the length of field lines. These difficulties are not present if the distance between field line footpoints is used: the function N cumulates locally the spatial variations of D. Moreover we have shown in Paper I that the regions where N takes unusually large values are the locations of strong flows leading to the breakdown of ideal MHD. We show in the Sect. 4 that these regions are also physically related with the places where magnetic energy is stored.

3.4. What is the thickness of Quasi-Separatrix layers ?

For $\varphi_P \geq 170^0$ a jump discontinuity in D is present along almost all the regions marked in Fig. 2a (see Fig. 4), at least until the numerical resolution limit ($\approx 10^{-14}$) is reached. The discontinuity disappears only close to the end of the regions drawn, where a smooth variation appears (Fig. 4b). For lower values of φ_P there is no discontinuity and the functions N, D, L, T take a standard shape when plotted with the scale-length of the drastic variation (Fig. 5). This is a structurally stable feature which can be used to characterise QSLs (rather than discontinuities). The maximum of the function N, N_{max}, is directly related to the thickness of QSL, δ (defined as the width of the function N at half-height). We have found for all the cases studied with four sources the simple relation:

$$N_{max}\delta \approx 0.2\,. \tag{4}$$

Since the shape of the funtion N is similar from one case to another, this means that the integral of N across a QSL is approximately preserved, which is natural because this integral is the difference in the position of field lines footpoints at both sides of the QSL.

As we have qualitatively seen in Sect. 3.1, the thickness of QSLs and the value of N_{max} depend also strongly on the size of the photospheric field concentrations (which are directly related to the depth d of the sources). We therefore investigate the relationship between N_{max}, d and φ_P when all the sources are at the depth d. We find that N_{max} is roughly a power of d (Fig. 5d) with

$$log_{10}N_{max} \approx a(\varphi_P)log_{10}d + b(\varphi_P), \tag{5}$$

where

$$a(\varphi_P) \approx 1.2(-2 + \varphi_P/(\varphi_P - 180)),$$

$$b(\varphi_P) \approx -1.6 - 10^{-4}(\varphi_P - 90)^2 + 0.26\varphi_P/(\varphi_P - 180).$$

The singularity for $\varphi_P = 180^0$ arises because of the presence of null points. As φ_P increases, not only N_{max} increases but the effect of more concentrated photospheric sources becomes stronger; very thin QSLs can be easily found by decreasing a little the size of photospheric field concentrations. For bipolar regions, thin QSLs can still be found with more concentrated photospheric fields (say 10^{-4} compared to the scale length of the whole magnetic configuration).

Typical active regions in the Sun have sizes of the order of 100 Mm, and so all the above dimensionless lengths have to be multiplied by 100 to express them in Mm; for example Eq. (4) gives $\delta \approx 20/N_{max}$ Mm. A thickness of say 10 m, where MHD laws should break down, is obtained for $N_{max} \geq 2.10^6$, which is realized mainly for $\varphi_P \geq 120^0$ if we limit ourselves to source concentration sizes greater than 1 Mm, but it is realized for nearly all configurations ($\varphi_P \geq 30^0$) if we consider flux concentrations as small as 0.1 Mm in size. In any case, flares observed in quadrupolar configurations do not show particularly different characteristics from those occurring in bipolar ones, except for different spatial locations of the brightenings (which

© European Southern Observatory • Provided by the NASA Astrophysics Data System

1996A&A...308..643D

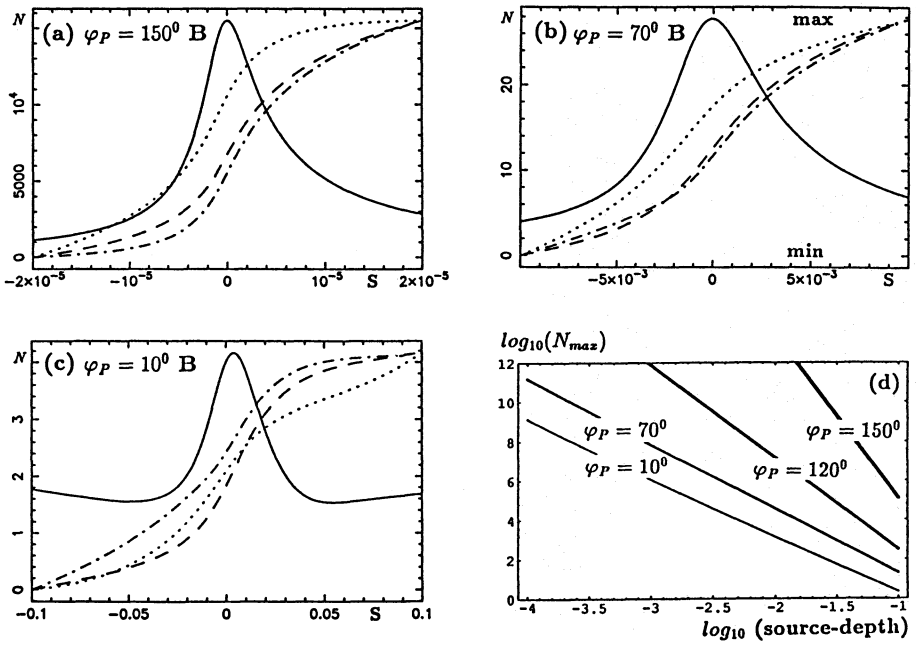


Fig. 5a–d. Width of quasi-separatrix layers for different values of φ_P. Plots are made along segments centred at point B (see Fig. 2) and perpendicular to the quasi-separatrix layer. The discontinuity of the three functions D, L, T (drawing convention as in Fig. 3) disappears for $\varphi_P \leq 170^0$ at all locations and the function N (full line) has a typical peaked shape. The maximum of N, N_{max}, decreases rapidly as the two bipoles become more parallel and as the source depth increases.

is explained by QSL positions). We will show in the next section that QSLs with thicknesses of few megameters are enough to develop concentrated currents with the observed sizes. These concentrated currents may provide the free magnetic energy to power flares.

4. Concentrated currents created by smooth photospheric motions

Several points are puzzling about the observations of photospheric currents. How are they generated ? Is it by photospheric motions, such as twisting or shearing motions ? or do flux tubes emerge twisted ? In the first case, why aren't coherent and intense photospheric motions, required to explain the observed intense currents, seen more often ? In the second case, why are the currents associated with flaring not observed moving to the positions of the H_α brightenings, but are rather always located in the regions where the kernels are present later.

The existence of regions of drastic change in field-line linkage in flaring magnetic configurations can overcome the above difficulties. We show below that concentrated currents are naturally formed by smooth photospheric motions at QSLs. The effect of photospheric displacements is amplified here. Two neighbouring field lines are subjected to different photospheric motions, since their opposite footpoints are separated by a great distance, and so these motions do not need to be localized and strong to produce the observed concentrated currents (for example, the global solar differential rotation can be enough).

Let us consider an initial potential magnetic field $\boldsymbol{B_0}$ that has no null points and no field line tangent to the photosphere, so that the mapping is continuous but it can change drastically at some places. For a given field line the distance between its photospheric footpoints is given by

$$\boldsymbol{d_0} = \int_{\text{field line}} \frac{\boldsymbol{B_0}}{B_0} dS \,. \tag{6}$$

The horizontal coordinates X_0, Y_0 of one of the field line footpoints (the one located in the positive flux region) can be used to label each field line. Because (X_0, Y_0) are constant for a field line, a vectorial basis ∇X_0, ∇Y_0 and ∇S_0 (which is parallel to $\boldsymbol{B_0}$) can be defined in every point along a line of force. The field $\boldsymbol{B_0}$ is orthogonal to both ∇X_0 and ∇Y_0 and it can be written, using unmatched Euler potentials, as

$$\boldsymbol{B_0} = b(X_0, Y_0) \quad \nabla X_0 \times \nabla Y_0 \,, \tag{7}$$

where $b(X_0, Y_0)$ is only a function of X_0, Y_0 because $div(\boldsymbol{B_0}) = 0$ (Stern 1970, Hesse & Schindler 1988).

A photospheric displacement (with line-tying) changing $\boldsymbol{d_0}$ to $\boldsymbol{d_0}+\boldsymbol{d_1}$ forces the field to evolve to a new equilibrium. Because the link between the displacement $\boldsymbol{d_1}$ and the perturbed magnetic field is nonlinear and nonlocal the full problem can only be solved numerically. To see simply the effect of the existence of drastic changes in field-line linkage in $\boldsymbol{B_0}$ on the current distribution created by the motions, we limit ourselves to small photospheric displacements ($d_1 << d_0$). Because the mapping is assumed to be continuous this induces small perturbations in the magnetic field and we expand it: $\boldsymbol{B} = \boldsymbol{B_0} + \boldsymbol{B_1} + ...$ The perturbed equilibrium equation to first order is simply:

$$\boldsymbol{J_1} \times \boldsymbol{B_0} = 0 \,. \tag{8}$$

We limit ourselves to the case of currents small enough that they do not change significantly the initial field so that the currents

© European Southern Observatory • Provided by the NASA Astrophysics Data System

1996A&A...308..643D

flow mainly parallel to the initial field. The relation between $\boldsymbol{d_1}$ and $\boldsymbol{B_1}$ reduces to

$$\boldsymbol{d_1} = \int_{\text{field line}} \frac{\boldsymbol{B_1} - (\boldsymbol{B_0}.\boldsymbol{B_1})\boldsymbol{B_0}/B_0^2}{B_0} dS\,. \tag{9}$$

For each field line, the photospheric displacement imposes an integral constraint on the perturbed field component which is orthogonal to $\boldsymbol{B_0}$.

The general solution of Eq. (8) is:

$$\boldsymbol{J_1} = a(X_0, Y_0) \quad \boldsymbol{\nabla} X_0 \times \boldsymbol{\nabla} Y_0\,. \tag{10}$$

To introduce this constraint in the photospheric displacement equation (Eq. (9)) we need first to compute the perturbed field $\boldsymbol{B_1}$ associated with $\boldsymbol{J_1}$. It is useful to express $\boldsymbol{B_1}$ in terms of the basis $\boldsymbol{\nabla} X_0$, $\boldsymbol{\nabla} Y_0$ and $\boldsymbol{\nabla} S_0$

$$\begin{aligned}\boldsymbol{B_1} &= U(X_0, Y_0, S_0)\boldsymbol{\nabla} X_0 + V(X_0, Y_0, S_0)\boldsymbol{\nabla} Y_0 \\ &+ W(X_0, Y_0, S_0)\boldsymbol{\nabla} S_0\,.\end{aligned} \tag{11}$$

The equation $\boldsymbol{J_1} = \boldsymbol{\nabla} \times \boldsymbol{B_1}$ gives the following relationship between the functions a, U, V, W

$$a = \frac{\partial V}{\partial X_0} - \frac{\partial U}{\partial Y_0}\,, \tag{12}$$

$$\frac{\partial U}{\partial S_0} = \frac{\partial W}{\partial X_0}\,, \tag{13}$$

$$\frac{\partial V}{\partial S_0} = \frac{\partial W}{\partial Y_0}\,. \tag{14}$$

The general solution of this system is

$$U = U_a(X_0, Y_0) + \frac{\partial P(X_0, Y_0, S_0)}{\partial X_0}\,, \tag{15}$$

$$V = V_a(X_0, Y_0) + \frac{\partial P(X_0, Y_0, S_0)}{\partial Y_0}\,, \tag{16}$$

$$W = \frac{\partial P(X_0, Y_0, S_0)}{\partial S_0}\,, \tag{17}$$

with

$$a(X_0, Y_0) = \frac{\partial V_a}{\partial X_0} - \frac{\partial U_a}{\partial Y_0}\,. \tag{18}$$

Then the first-order perturbed magnetic field becomes:

$$\begin{aligned}\boldsymbol{B_1} &= U_a(X_0, Y_0)\boldsymbol{\nabla} X_0 + V_a(X_0, Y_0)\boldsymbol{\nabla} Y_0 \\ &+ \boldsymbol{\nabla} P(X_0, Y_0, S_0)\,.\end{aligned} \tag{19}$$

The functions U_a, V_a and P are determined from the constraint $div(\boldsymbol{B_1}) = 0$ and Eq. (9) becomes:

$$\begin{aligned}\boldsymbol{d_1} &= U_a(X_0, Y_0) \int_{\text{f.l.}} \frac{\boldsymbol{\nabla} X_0}{B_0} dS + V_a(X_0, Y_0) \int_{\text{f.l.}} \frac{\boldsymbol{\nabla} Y_0}{B_0} dS \\ &+ \int_{\text{f.l.}} \left(\frac{\partial P}{\partial X_0} \frac{\boldsymbol{\nabla} X_0}{B_0} + \frac{\partial P}{\partial Y_0} \frac{\boldsymbol{\nabla} Y_0}{B_0} \right) dS\,.\end{aligned} \tag{20}$$

In the first two right-hand terms of Eq. (20), the integrals depend only on the initial equilibrium field $\boldsymbol{B_0}$. They change drastically at QSL locations and lead to a drastic variation of the functions U_a, V_a for a smooth displacement $\boldsymbol{d_1}$, unless the last term in Eq. (20) balances exactly the variation imposed by the first two integrals. This is unlikely to be the case in general because the last term contains different functions inside the integral. In order that this term compensates exactly the drastic change imposed by the first two, a particular relationship between the functions U_a, V_a, P is needed which is in general incompatible with the constraint $div(\boldsymbol{B_1}) = 0$. We can go further in the analysis in the particular case when the function P is independent of S_0. This means that we neglect the variation of $\boldsymbol{B_1}$ along field lines. Then $\boldsymbol{B_1}$ is perpendicular to $\boldsymbol{B_0}$ and Eq. (9) reduces to:

$$\begin{aligned}\boldsymbol{d_1} &= \left(U_a(X_0, Y_0) + \frac{\partial P}{\partial X_0} \right) \int_{\text{f.l.}} \frac{\boldsymbol{\nabla} X_0}{B_0} dS \\ &+ \left(V_a(X_0, Y_0) + \frac{\partial P}{\partial Y_0} \right) \int_{\text{f.l.}} \frac{\boldsymbol{\nabla} Y_0}{B_0} dS\,.\end{aligned} \tag{21}$$

The integrals are now functions only of the initial magnetic configuration. At QSLs the integrals in Eq. (21) change their values drastically and, unless the photospheric displacement $\boldsymbol{d_1}$ has exactly this kind of variation, the functions U_a, V_a and P should compensate these drastic changes. This implies the generation of concentrated currents since $a(X_0, Y_0) = \partial V_a/\partial X_0 - \partial U_a/\partial Y_0$. Currents are in fact created throughout the active region, but they are much more intense where neighbouring field lines have their opposite feet widely separated. However, due to its small thickness the quasi-separatrix is a privileged location for the presence of high current densities. So any smooth photospheric displacement can create concentrated currents at quasi-separatrices. Of course we still need to solve the full problem so as to know precisely the distribution of currents for given photospheric motions, but from this discussion we know that the most intense currents are only present in small fractions of the active region. As we have shown in previous papers it is at these locations that chromospheric flares are observed.

The formation of concentrated currents does not require the presence of particular photospheric motions. This explains why no specific pattern of displacement has been observed in flaring regions. Any smooth photospheric motion creates concentrated currents at the places where the energy is later released; we can invoke emerging flux, shearing or twisting motions or simply magnetic field evolution on the scale of the active region. As the current density increases, rapid energy release via reconnection can start. This can happen either because the resistivity is increased to anomalous values (when the threshold for a current-driven instability is exceeded, e.g. when the drift velocity of the current becomes larger than the ion-acoustic speed) or because the magnetic field becomes too twisted (e.g. kink instability driving reconnection), but the precise mechanism has yet to be found. Homologous flares are natural in such a scenario: after one flare the vertical photospheric field is essentially the same as it was before the flare, so the field-line linkage and the currents are formed at nearly the same place. The recurrence of homologous flares may continue until the photospheric field distribution has changed.

© European Southern Observatory • Provided by the NASA Astrophysics Data System

1996A&A...308..643D

5. Conclusions

In the previous papers we have analyzed the magnetic topology of flaring active-regions. Our results show that solar flares represent a conversion of magnetic energy by magnetic reconnection. We have found that Hα brightenings are invariably located on part of the region where the computed separatrices intersect the photosphere and are linked in pairs by magnetic field lines. The 3D coronal magnetic field was computed extrapolating the field of a set of subphotospheric magnetic sources, instead of using a more conventional extrapolation technique. The physical parameters of the sources were chosen to match as closely as possible the observed photospheric field. The topology was defined by the linkage between these sources (SM). Because flares are mainly coronal events, with marginal effects on the photosphere and none on subphotospheric layers, the properties of flaring active regions should be deduced from the magnetic field configuration above the photosphere. Since the starting point of our 3D topological analysis we have been conscious of the intrinsic limitations of the SM. The design of a new method, both closer to reconnection theory and to the observations, was not easy because several properties of 2D or $2\frac{1}{2}$D configurations cannot be generalised to 3D. Several attempts, some of which are summarised below, have failed but they were a useful training to understand the characteristics of 3D configurations.

The simplest way to find the topology of 2D configurations is to locate the magnetic null points and after that to derive the separatrices. A null point in 2D configurations is a separator. However, in 3D configurations a separator cannot be found through a local analysis of the magnetic field as in 2D (see the Appendix in this paper) ! However, the null points can still be found locally and after that the separator joining them, but many observed flaring configurations have no nulls at all above the photosphere ! Looking locally at the field line behaviour in a plane perpendicular to the field, Priest & Forbes (1989) showed that they have an X-type topology, but the location of the line where an X-structure is present changes its position as the orientation of the plane is modified ! They called such a line a "potential singular field line" and they showed that there is a continuum of such lines. They proposed that the imposed boundary flows select the particular line on which reconnection occurs. In our observational studies we have however located the flare brightenings on separatrices (computed with the SM) without any reference to the plasma flow. Therefore, observations show that the energy release is located in regions defined only by the magnetic field properties. This define the spatial location of the breakdown of ideal MHD in the 3D magnetic reconnection theory of Hesse & Schindler (1988), emphasizing the importance of the magnetic topology but in a wider sense than was thought before.

Well-defined separatrices can be found with the SM because there is a clear difference between sources even if they have the same polarity. Can we separate observed photospheric field concentrations in a similar way ? For field concentrations having the same sign there is no way to justify a division, unless the field has a negligible magnitude between field concentrations though there are several observed examples where it is of the order of several hundred Gauss. Another way to gain some insight into the topology is to look for discontinuities in functions such as the field line length (L) or the distance (D) between field line footpoints. Lau (1993) showed that it is better to use the delay function (T) because it has a logarithmic singularity, while L or D have only a jump discontinuity. However, this is valid only for magnetic configurations having a separator above the photosphere. For more general configurations we show that the delay function (T) has the same smooth behaviour as L and D. A method looking only for discontinuities in functions L, D or T would exclude most of the configurations that are observed to flare. From the studied flaring regions, no evidence has been found that field lines tangent to the photosphere or chromosphere play a role in flares.

With this background, we have looked at the field-line linkage above the photosphere in simple configurations representative of the observed ones. In particular, we have defined a function (see also Paper I) called N that characterises the regions where the field-line linkage changes drastically, and we have named those regions quasi-separatrix layers. They are the generalization of the well-known separatrices. We have developed an algorithm to determine the location of quasi-separatrix layers called QSLM. While we limit ourselves in this paper to simple potential configurations, the method is designed for any kind of magnetic field evolving quasi-statically; the magnetic field representation can be of any kind (discrete sources, finite differences, finite elements). In the limit of infinitely concentrated photospheric fields, we have shown that N becomes infinitely concentrated all along the position of the separatrices computed with the SM. When the photospheric field concentrations have finite sizes, the locations of the highest values of N are near the separatrices computed with the SM. In most of the magnetic configurations analysed, we have no well-defined surfaces separating connectivity cells as with the SM but very flat volumes (QSLs). The notion of separatrices disappears in general; it remains only when null points are present above the photosphere or if some field lines are tangent to the boundary.

The QSLM defines regions more restricted in length than the SM. We have found two regions showing a steep gradient in field-line linkage in bipolar configurations and four in quadrupolar ones (excluding the parts where field lines are tangent to the photosphere). The four regions are linked two by two by field lines, as in 2D quadrupolar regions; these four regions are gathered in pairs in bipolar cases to give two folded regions (see Figs. 1 and 2). This evolution of the connectivity with φ_P explains the observation of four flare brightenings (sometimes only three are visible) in antiparallel configurations and only two in bipolar ones (Mandrini et al. 1991, 1993, 1995, Démoulin et al. 1993, 1994b, Van Driel-Gesztelyi et al. 1994). However, the field-line linkage is not generally discontinuous in these regions as was thought before. The more concentrated the photospheric field is and the more quadrupolar the configuration is, the thinner the QSLs are.

We have shown that the QSLs are privileged regions for the formation of concentrated currents. A general photospheric

© European Southern Observatory • Provided by the NASA Astrophysics Data System

1996A&A...308..643D

motion creates not only distributed currents in the whole configuration, whose locations depend on the velocity pattern, but also strong and concentrated ones at QSLs. We have proved this only in the case of initial potential configurations but we conjecture that it extends to any kind of magnetic equilibrium. This explains why the observed vertical currents are observed more concentrated than the vertical photospheric field. It also answers the question: why are the observed currents always found on or at the border of flare brightenings even if the magnetogram used was taken several hours before the flare ? The currents are not evolving towards the reconnection region, they are mainly formed where it will occur. In Paper I we have also shown that 3D magnetic reconnection, in the absence of null points, may occur at QSLs with a breakdown of ideal MHD and a change of connectivity of plasma elements. This happens even when a smooth boundary motion is imposed. The consequence of this motion is that the field line velocity greatly exceeds the possible plasma velocity (an upper bound being typically of the order of the Alfven velocity) and an electric field component is produced along the magnetic field in the layer so that field lines flip rapidly through the plasma. Therefore, the regions defined by the QSLM seem to gather all the required prerequisites for flaring: energy can be stored and released there !

Acknowledgements. P.D., J.C.H. and C.H.M. acknowledge financial support from the CONICET (Argentina) and CNRS (France) through their Argentina/France cooperative science program, while E.R.P. thanks the UK PPARC for financial support. We thank Slava Titov and Bert Van den Oord for fruitful discussions on this paper. C.H.M. thanks the hospitality of the group at DASOP during her stay there.

Appendix A: can a local criterion define the magnetic topology ?

The QSLM requires the computation of thousands of field lines to determine the field topology. It requires also an automatic algorithm to converge on the places of drastic change in field-line linkage. This can be avoided in the particular case of field lines tangent to the photosphere because a local criterion is sufficient (see Bungey et al. 1995 for example). Is it possible in other cases ? When the field-line linkage changes smoothly there is no possible local criterion because all the neighbouring field lines have the same linkage, if they are close enough. However, in cases where the field-line linkage is discontinuous, we may think that a local criterion is possible (as for the null points present in the configuration). The object of this Appendix is to show that we cannot fulfil such a hope.

If such a local criterion exists it should be linked to the local behaviour of the magnetic field: consequently, we expand locally the magnetic field $\boldsymbol{B}(\boldsymbol{r})$ to the first order in $\boldsymbol{dr} = \boldsymbol{r} - \boldsymbol{r_0}$

$$\boldsymbol{B}(\boldsymbol{r}) = \boldsymbol{B}(\boldsymbol{r_0}) + M_0 \boldsymbol{dr} + O(\boldsymbol{dr}^2)\,, \qquad (A1)$$

where M_0 is the Jacobian matrix computed at $\boldsymbol{r_0}$. The behaviour of the field lines near $\boldsymbol{r_0}$ is determined by the eigenvalues λ_i, $i = 1, 3$ and the corresponding eigenvectors $\boldsymbol{e_i}$ of the matrix M_0. In the basis of the eigenvectors $\boldsymbol{e_i}$, the equation for a field line is simply

$$\frac{dx_1}{b_1 + \lambda_1 x_1} = \frac{dx_2}{b_2 + \lambda_2 x_2} = \frac{dx_3}{b_3 + \lambda_3 x_3}\,, \qquad (A2)$$

where $\boldsymbol{B}(\boldsymbol{r_0}) = \sum_{i=1}^{3} b_i \boldsymbol{e_i}$. Field lines diverge locally from each other if the zeroth-order field $\boldsymbol{B}(\boldsymbol{r_0})$ is parallel to one of the eigenvectors ($\boldsymbol{e_1}$ say) and if the eigenvalues associated with the other two eigenvectors have opposite signs. That is to say,

$$b_2 = b_3 = 0 \qquad (A3)$$

and

$$\lambda_2 \lambda_3 < 0\,.$$

This provides a local criterion. It looks like a logical extension to 3D of the 2D X-type topology. Let us notice that it is not obvious that, for the global configuration, the local divergence of the field lines would imply a discontinuous field-line linkage.

The curve defined by Eq. (A3) is not necessarily a tangent to the eigenvector $\boldsymbol{e_1}$ and therefore to the magnetic field. It is not a field line in general. This shows that this attempt to find a local criterion has failed because it is known that a separator is a field line (see e.g., Baum and Bratenahl 1980, Gorbachev and Somov 1988). The curve represented by Eq. (A3) describes exactly the position of the separator when the field is always parallel to that curve, i.e. in the particular case of a configuration invariant by translation ($2\frac{1}{2}$D).

A simple example can help us to understand why the location of a separator is a global property of the magnetic field configuration. Let us take a general magnetic configuration (called $\boldsymbol{B_1}$) having two null points. The separator is the field line linking these two null points. Let us add near one of these null points (called N_1) a magnetic field (called $\boldsymbol{B_2}$) with finite spatial extension: it is supposed to be non-zero only in a finite volume V around N_1 (an example is the field created by a solenoid). In the field configuration $\boldsymbol{B_1} + \boldsymbol{B_2}$ the position of N_1 is changed, and so does the position of the separator, while the magnetic field outside the volume V remains the same. Any local criterion used to locate the separator gives the same position for both configurations, $\boldsymbol{B_1}$ and $\boldsymbol{B_1} + \boldsymbol{B_2}$, outside the volume V. It shows that such a local criterion cannot exist. Thus, exept in the particular case of field lines tangent to the boundary, the topology of magnetic configurations can only be deduced by a global criterion, such as the computation of field lines and their linkage. This obviously extends to configurations with a field-line linkage that is not strictly discontinuous and so has no separator.

References

Amari T. 1991, in *Advances in Solar System Magnetohydrodynamics*, Eds. E.R Priest, A. W. Hood., Cambridge University Press, p. 173
Baum P. & Bratenahl A. 1980, Solar Phys. 67, 245
Billinghurst M.N., Craig I.J.D. & Sneyd A.D. 1993, A&A 279, 589
Bungey T.N., Titov, V.S. & Priest, E.R. 1995, A&A in press
Démoulin P. 1994, Proceedings of "Advances in Solar Physics", eds. G. Belvedere, W. Mattig and M. Rodono, Springer-Verlag, p. 121

© European Southern Observatory • Provided by the NASA Astrophysics Data System

1996A&A...308..643D

Démoulin P., Hénoux J.C. & Mandrini C.H. 1992, Solar Phys. 139, 105
Démoulin P., Hénoux J.C. & Mandrini C.H. 1994a, A&A 285, 1023
Démoulin P., Mandrini C.H., Rovira M.G., Hénoux J.C. & Machado M.E. 1994b, Solar Phys. 150, 221
Démoulin P., Van Driel-Gesztelyi L., Schmieder B., Hénoux J.C., Csepura G. & Hagyard M.J. 1993, A&A 271, 292
Gorbachev V.S. & Somov B.V. 1988, Solar Phys. 117, 77
Gorbachev V.S. & Somov B.V. 1989, Sov. Astron. 33, 1, 57
Hesse M. & Schindler K. 1988, JGR 93, A6, 5559
Heyvaerts, J., Priest, E.R. and Rust, D.M. 1977, ApJ 216, 123.
Karpen J.T., Antiochos S.K. & DeVore C.R. 1990, ApJ 356, L67
Karpen J.T., Antiochos S.K. & DeVore C.R. 1991, ApJ 382, 327
Lau Y.T. 1993, Solar Phys. 148, 301
Lau Y.T. & Finn J.M. 1990, ApJ 350, 672
Low B.C. 1987, ApJ 323, 358
Low B.C. 1992, A&A 253, 311
Low B.C. & Wolfson R. 1988, ApJ 324, 574
Mandrini C.H., Démoulin P., Hénoux J.C. & Machado M.E. 1991, A&A 250, 541
Mandrini C.H., Démoulin P., Rovira, M.G., De la Beaujardiere, J.F., & Hénoux J.C. 1995, A&A in press
Mandrini C.H., Rovira M.G., Démoulin P., Hénoux J.C., Machado M.E. & Wilkinson L.K. 1993, A&A 272, 609
Priest E.R. & Forbes T.G. 1989, Solar Phys. 119, 211
Priest E.R. and Démoulin P. 1995, JGR in press
Priest, E.R. and Forbes, T.G. 1989, Solar Phys. 119, 211
Priest, E.R. and Forbes, T.G. 1990, Solar Phys. 126, 319
Priest E.R. & Forbes T.G. 1992a, JGR 97, A2,1521
Priest E.R. & Forbes T.G. 1992b, JGR 97, A11,16757
Priest, E.R. and Titov, V.S. 1995, Phil. Trans. of Roy. Soc., submitted
Schindler, K., Hesse, M. and Birn, J. 1988, JGR 93, 5547
Somov B.V. 1986, A&A 163, 210
Somov B.V. 1992, Solar Flares, Springer Verlag
Stern D.P. 1970, Am. J. Phys. 38, 494
Van den Oord G.H.J. 1993, Proc. of COSPAR meeting, in Advances in Space Research, 13, 9,143
Van Driel-Gesztelyi L., Hofmann A., Démoulin P., Schmieder B. & Csepura G. 1994, Solar Phys. 149, 309
Vekstein G.E. & Priest E.R. 1992, ApJ 384, 333
Vekstein G.E., Priest E.R. & Amari T. 1991, A&A 243, 492
Wolfson R. 1989, ApJ 344, 471

This article was processed by the author using Springer-Verlag LaTeX A&A style file version 3.

© European Southern Observatory • Provided by the NASA Astrophysics Data System